RNA-binding protein YTHDF3 suppresses interferon-dependent antiviral responses by promoting FOXO3 translation

Yuan Zhang[a], Xin Wang[a], Xiao Zhang[a], Jiaming Wang[a], Yuanwu Ma[b], Lianfeng Zhang[b], and Xuetao Cao[a,c,d,1]

[a]Department of Immunology & Center for Immunotherapy, Institute of Basic Medical Sciences, Chinese Academy of Medical Sciences, School of Basic Medicine Peking Union Medical College, 100005 Beijing, China; [b]Key Laboratory of Human Disease Comparative Medicine, Ministry of Health, Institute of Laboratory Animal Science, Chinese Academy of Medical Sciences, 100021 Beijing, China; [c]National Key Laboratory of Medical Immunology, Institute of Immunology, Second Military Medical University, 200433 Shanghai, China; and [d]College of Life Science, Nankai University, 300071 Tianjin, China

Edited by Robert L. Coffman, Dynavax Technologies, Berkeley, CA, and approved December 4, 2018 (received for review July 21, 2018)

IFN–stimulated genes (ISGs) are essential effectors of the IFN-dependent antiviral immune response. Dysregulation of ISG expression can cause dysfunctional antiviral responses and autoimmune disorders. Epitranscriptomic regulation, such as N^6-methyladenosine (m^6A) modification of mRNAs, plays key roles in diverse biological processes. Here, we found that the m^6A "reader" YT521-B homology domain-containing family 3 (YTHDF3) suppresses ISG expression under basal conditions by promoting translation of the transcription corepressor forkhead box protein O3 (FOXO3). YTHDF3 cooperates with two cofactors, PABP1 and eIF4G2, to promote FOXO3 translation by binding to the translation initiation region of FOXO3 mRNA. Both the YTH and the P/Q/N-rich domains of YTHDF3 were required for FOXO3 RNA-binding capacity, however, METTL3-mediated m^6A modification was not involved in the process observed. Moreover, YTHDF3$^{-/-}$ mice had increased ISG levels and were resistant to several viral infections. Our findings uncover the role of YTHDF3 as a negative regulator of antiviral immunity through the translational promotion of FOXO3 mRNA under homeostatic conditions, adding insight into the networks of RNA-binding protein-RNA interactions in homeostatically maintaining host antiviral immune function and preventing inflammatory response.

YTHDF3 | interferon | innate response | antiviral immunity | FOXO3

Epitranscriptomic regulation plays a vital role in gene expression (1), and it is becoming increasingly clear that the epitranscriptome and its executors are widely involved in physiological and pathological conditions. N^6-methyladenosine (m^6A) is the most abundant internal and reversible mRNA modification in eukaryotes and regulates RNA metabolism, folding, export, splicing, and translation. m^6A is a key regulator in the differentiation of embryonic stem cells, spermatogenesis, neurodevelopment, cardiovascular disease, leukemia, and glioblastoma (2). In addition, m^6A modulates the immune system, influencing T cell homeostasis, type I IFN production, and viral replication (3–5). As a result, epitranscriptomics have emerged as a promising area of research with wide-reaching potential. Nevertheless, the specific functions of epitranscriptome in innate immunity and inflammation remain elusive.

Type I IFNs play vital roles in antiviral innate responses. With the engagement of the IFN-α/β receptor (IFNAR), type I IFNs initiate a signaling cascade through the Janus kinase signal transducer and activator of transcription (JAK-STAT) pathway, resulting in transcription of thousands of IFN–stimulated genes (ISGs) (6, 7). Autocrine type I IFN signaling is maintained homeostatically at low levels in the absence of infection and plays a critical role in hematopoietic stem cell development, immune cell function, autoimmune diseases, and antitumor and antiviral responses (7). Dysregulation of type I IFN responses can cause deficiencies in antiviral immunity or result in autoimmune diseases (8). Therefore, the homeostasis of type I IFN responses is pivotal for host health and is tightly regulated at both transcriptional and post-translational levels. At the transcriptional level, the transcription factor T-bet functions as a repressor of type I IFN-stimulated genes (9). At the post-translational level, IFN-α-dependent antiviral immunity is amplified by methyltransferase SETD2, which catalyzes both the methylation of STAT1 on K525 and the trimethylation of histone H3K36 at promoter regions of ISGs (10). However, how ISG expression is regulated under homeostatic conditions is less clear.

Selective regulation of translation controls the abundance of proteins, including those that determine innate and adaptive immune responses (11). Co- and post-transcriptional modifications of mRNAs, such as m^6A, regulate translation accuracy and efficiency, allowing cells to rapidly and dynamically reprogram gene expression under determined conditions. m^6A realizes its function primarily by recruiting different types of RNA-binding proteins, including the YT521-B homology (YTH) domain-containing proteins, eukaryotic initiation factor 3 (eIF3), and insulinlike growth factor 2 mRNA-binding proteins (IGF2BPs), which subsequently direct multiprotein complexes to selectively bind to m^6A-containing transcripts (12). The YTH domain-containing proteins are best characterized as m^6A "readers." Among these, YTH domain-containing family 1 (YTHDF1) promotes translation efficiency by

Significance

Type I IFN signaling is maintained under homeostatic conditions, which plays a crucial role in antiviral immunity. Epigenetic regulation of innate immunity and inflammation attracts much attention now. However, the underlying mechanisms need further investigation. Here, we demonstrate that N^6-methyladenosine (m^6A) "reader" YT521-B homology domain-containing family 3 (YTHDF3) selectively inhibits IFN-stimulated gene expression under basal conditions by binding to the translation initiation region of the transcription corepressor forkhead box protein O3 (FOXO3) mRNA and promoting its translation. Unexpectedly, the capacity of YTHDF3 for binding FOXO3 mRNA is independent of METTL3-mediated m^6A modification. Our paper adds a view of YTHDF family proteins in the control of IFN antiviral responses. Overall, the roles of RNA-binding proteins and their RNA targets with certain modifications in inflammation and autoimmune diseases need further identification.

Author contributions: X.C. designed research; Y.Z., X.W., X.Z., J.W., Y.M., and L.Z. performed research; Y.Z. and X.C. analyzed data; and Y.Z. and X.C. wrote the paper.

The authors declare no conflict of interest.

This article is a PNAS Direct Submission.

[1]To whom correspondence should be addressed. Email: caoxt@immunol.org.

This article contains supporting information online at www.pnas.org/lookup/suppl/doi:10.1073/pnas.1812536116/-/DCSupplemental.

Published online December 27, 2018.

binding m^{6}A-modified mRNA, whereas YTHDF2 decreases mRNA stability by recruiting the CCR4-NOT deadenylase complex (13–15). YTHDF3 facilitates translation and decay of m^{6}A-modified mRNAs through cooperation with YTHDF1 and YTHDF2 (16, 17). However, the role for YTHDF family proteins in immune responses remains to be elucidated.

Although the m^{6}A modification has been identified in viral RNA decades ago, it has only now become evident that viral infections affect the dynamics of both host and viral m^{6}A. Several studies reported that YTHDF family proteins were involved in the viral life cycle, including the hepatitis C virus (18), the Zika virus (19), the Influenza A virus (20), and Kaposi's sarcoma-associated herpesvirus (21). YTHDF proteins have been implicated in human immunodeficiency virus infection, although the results are somewhat conflicting (22–24). m^{6}A modification has also been shown to play a crucial role in discriminating self- and non-self-RNA (25, 26). Therefore, an interesting open question is whether the YTHDF family proteins directly regulate the host innate antiviral response.

In this paper, we screened YTHDF proteins and identified YTHDF3 as the only negative regulator of ISG expression under homeostatic conditions. YTHDF3-deficient cells had broad antiviral activity against RNA and DNA viruses, and this activity was mediated by the IFNAR1 signaling pathway. However, METTL3-mediated m^{6}A modification unexpectedly appears not to be involved in this process. We found that YTHDF3 acted cooperatively with eIF4G2 and PABP1 and promoted translation of the repressive transcription factor, forkhead box protein O3 (FOXO3) through binding to the translation initiation region of FOXO3 mRNA. Thus, YTHDF3 is vital to homeostatically sustain ISG transcription and host antiviral immunity.

Results

YTHDF3 Promotes Viral Replication. To investigate the role of the YTHDF family of proteins in host antiviral immune responses, we transfected mouse peritoneal macrophages with pools of four small interfering RNAs (siRNAs) to target each of these individual YTHDF genes. Fluorescence microscopy showed that only siYTHDF3 significantly reduced the levels of green fluorescent protein- (GFP-) tagged vesicular stomatitis virus (VSV) (Fig. 1*A* and *SI Appendix*, Fig. S1*A*), whereas YTHDF1 and YTHDF2 knockdown had barely any effect (Fig. 1*A* and *SI Appendix*, Fig. S1*A*). Next, we generated YTHDF-deficient RAW264.7 cells by CRISPR-Cas9. Similar to the above results, we found that VSV-GFP infection was only reduced in YTHDF3$^{-/-}$ RAW264.7 cells (*SI Appendix*, Fig. S1 *C* and *D*). Consistently, the abundance of VSV RNA reduced after YTHDF3 silencing and in YTHDF3$^{-/-}$ RAW264.7 cells (Fig. 1*B* and *SI Appendix*, Fig. S1*E*). We also detected VSV-glycoprotein (-G) levels and measured VSV titers (Fig. 1*B* and *SI Appendix*, Fig. S1 *B*, *E*, and *F*), both of which decreased in the YTHDF3-knockdown cells and YTHDF3$^{-/-}$ RAW264.7 cells.

To determine whether YTHDF3 affected host susceptibility to other viruses, we infected mouse macrophages with encephalomyocarditis virus (EMCV) and herpes simplex virus type 1 (HSV-1). Similar to the VSV results, the copy number of EMCV and HSV-1 were lower under siYTHDF3 in peritoneal macrophages and in YTHDF3$^{-/-}$ RAW264.7 cells (Fig. 1 *C* and *D* and *SI Appendix*, Fig. S1 *G* and *H*). Together, these results demonstrate that YTHDF3-silenced or deficient cells are resistant to virus infection with several types of RNA and DNA viruses.

YTHDF3-Mediated Down-Regulation of ISG Expression Is Dependent on Autocrine Type I IFN Signaling. We next explored the potential regulatory roles of YTHDF3 in antiviral immunity. To determine whether YTHDF3 expression could be regulated in response to virus infection or IFN-β stimulation, we treated mouse peritoneal macrophages with VSV, EMCV, HSV-1, Sendai virus, or IFN-β.

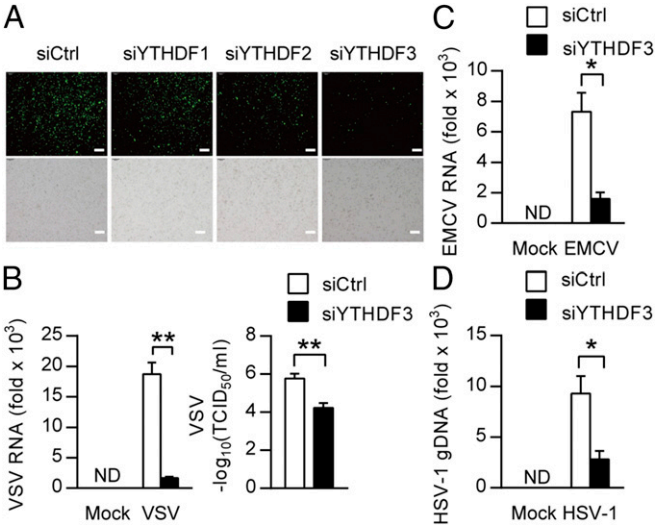

Fig. 1. Silencing of YTHDF3 inhibits viral infection in macrophages. (*A*) Fluorescence (*Top*) and bright field (*Bottom*) microscopy of mouse peritoneal macrophages transfected with siControl (siCtrl), siYTHDF1, siYTHDF2, or siYTHDF3, followed by infection for 12 h with VSV-GFP (green fluorescence) multiplicity of infection [(MOI), 1]. (Scale bars, 100 μm.) (*B*) qPCR analysis of VSV-RNA and VSV titers detection in the supernatant of mouse peritoneal macrophages transfected with siCtrl and siYTHDF3, followed by infection for 12 h with VSV (MOI, 1). (*C*) qPCR analysis of EMCV RNA in mouse peritoneal macrophages transfected with siCtrl or siYTHDF3, infected for 12 h with EMCV. (*D*) qPCR analysis of HSV-1 genomic DNA (gDNA) in mouse peritoneal macrophages transfected with siCtrl or siYTHDF3, infected for 12 h with HSV-1. Data are representative of three independent experiments [error bars (*B–D*), SD]. ND, not detectable. $*P < 0.05$, $**P < 0.01$ (two-tailed Student's *t* test).

Both mRNA and protein-expression levels of YTHDF3 were markedly reduced after virus infection or IFN-β treatment (*SI Appendix*, Fig. S3 *A* and *B*). Next, we investigated the influence of YTHDF3 on antiviral effector gene expression. We examined gene-expression profiles in YTHDF3$^{+/+}$ and YTHDF3$^{-/-}$ RAW264.7 cells by RNA-Seq. Five-hundred-ninety-two differentially expressed genes were enriched in the biological process in innate immune responses, type I IFN signaling pathways, and response to the virus by gene ontology analysis (*SI Appendix*, Fig. S2*A*). The most highly enriched up-regulated pathways revealed a signature indicative of innate antiviral responses to viral infection, such as the pattern recognition receptor signaling pathway and virus infection (*SI Appendix*, Fig. S2*B*). We also found that the expression of a subset of ISGs was significantly increased under basal conditions in YTHDF3$^{-/-}$ RAW264.7 cells compared with their wild-type (WT) counterparts (Fig. 2*A* and *SI Appendix*, Table S1). The induction of these ISG expressions was confirmed by qPCR analysis in uninfected YTHDF3$^{-/-}$ RAW264.7 cells and up-regulated expression of several ISGs, such as IFIT1, CXCL10, MX1, and OAS1a was detected (Fig. 2*B*). The levels of IFN-β mRNA were unaffected (*SI Appendix*, Fig. S2*D*). Similarly, siRNA-mediated knockdown of YTHDF3 also resulted in considerable induction of basal ISG mRNA expression (*SI Appendix*, Fig. S3*C*), which suggested that the lack of YTHDF3 function alone was sufficient to initiate an antiviral state in macrophages. Collectively, these data demonstrate that YTHDF3 is a physiological feedback regulator of ISG expression and viral infection and type I IFN-mediated inducible down-regulation of YTHDF3 may facilitate an antiviral state in host cells.

To further confirm that the ISG-activation signature was specific to the loss of YTHDF3 function, we performed rescue experiments using FLAG-YTHDF3 in YTHDF3$^{-/-}$ RAW264.7 cells. Stable expression of full-length YTHDF3 in YTHDF3$^{-/-}$ RAW264.7 cells reduced mRNA expression of IFIT1 and IRF7 (*SI Appendix*, Fig. S2*D*). Furthermore, the reintroduction of

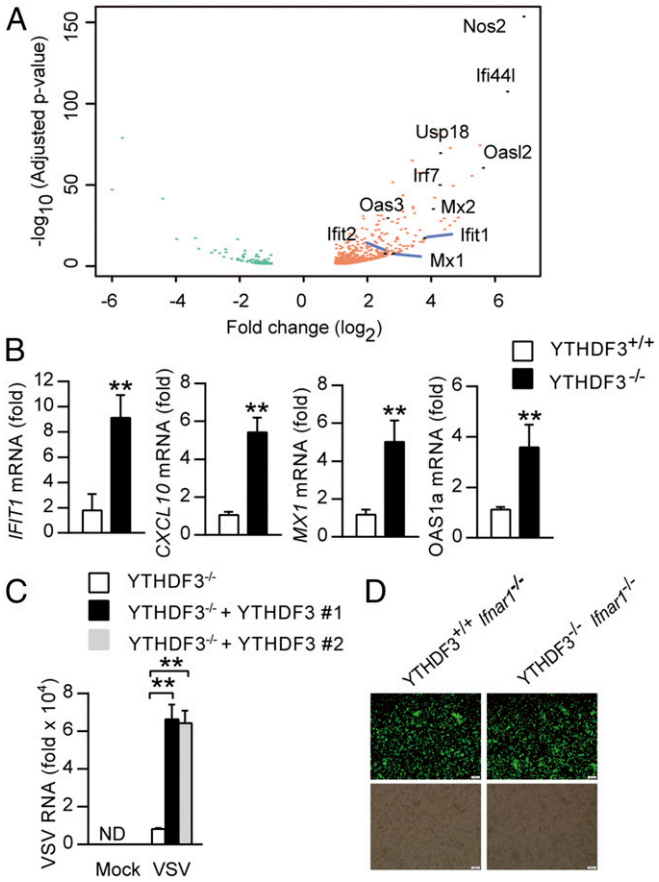

Fig. 2. YTHDF3-mediated negative regulation of ISG expression and antiviral response is dependent on IFNAR1 signaling in macrophages. (*A*) Volcano plots displaying the fold change and adjusted *P* value of differentially expressed genes (≥twofold change and adjusted *P* value < 0.05) in YTHDF3$^{-/-}$ RAW264.7 cells compared with YTHDF3$^{+/+}$ RAW264.7 cells. Black-coded genes correspond to the text. (*B*) qPCR analysis of selected ISGs in YTHDF3$^{+/+}$ and YTHDF3$^{-/-}$ RAW264.7 cells. (*C*) qPCR analysis of VSV RNA in YTHDF3$^{-/-}$ RAW264.7 cells and YTHDF3$^{-/-}$ RAW264.7 cells with stable expression of FLAG-YTHDF3. (*D*) Fluorescence (*Top*) and bright field (*Bottom*) microscopy of YTHDF3$^{+/+}$ *Ifnar1*$^{-/-}$ and YTHDF3$^{-/-}$ *Ifnar1*$^{-/-}$ mouse peritoneal macrophages infected for 12 h with VSV GFP (green fluorescence) (MOI, 1). (Scale bars, 100 μm.) Data are representative of three independent experiments [error bars (*B* and *C*), SD]. $^{**}P < 0.01$ (two-tailed Student's *t* test). ND, not detectable.

YTHDF3 into YTHDF3$^{-/-}$ RAW264.7 cells rendered these less resistant to VSV GFP compared with the parent cells (*SI Appendix*, Fig. S3*D*) and restored both VSV RNA (Fig. 2*C*) and VSV-G protein expression (*SI Appendix*, Fig. S3*E*). These data indicate that YTHDF3 selectively down-regulates ISG expression and enhances virus infection.

To further investigate the in vivo biological role of YTHDF3, we generated YTHDF3-deficient mice by deleting exon 4 with the CRISPR/Cas9 system (*SI Appendix*, Fig. S4). These YTHDF3$^{-/-}$ mice were viable and normal in size compared with their WT littermates. The percentages of lymphocytes and myeloid cells among the splenocytes of YTHDF3$^{-/-}$ mice were similar to those of WT mice (*SI Appendix*, Fig. S5), indicating that YTHDF3 is not involved in the development of myeloid cells. YTHDF3$^{-/-}$ bone marrow-derived macrophages (BMDMs) showed higher ISG-expression levels than YTHDF3$^{+/+}$ BMDMs (*SI Appendix*, Fig. S2*C*), but both IFN-α and IFN-β mRNA expressions were unaffected (*SI Appendix*, Fig. S2*C*). Following infection with VSV, the abundance of both VSV RNA and VSV-G protein in YTHDF3$^{-/-}$ BMDMs was much lower compared with that in WT cells (*SI Appendix*, Fig. S3 *F* and *H*). We also observed much lower levels of VSV proteins in YTHDF3$^{-/-}$ bone marrow-derived dendritic cells and YTHDF3$^{-/-}$ mouse embryonic fibroblasts after VSV infection than that in WT cells (*SI Appendix*, Fig. S3 *G* and *I*).

We next analyzed whether ISG activation and enhanced antiviral response caused by YTHDF3 loss were dependent on the IFNAR1 pathway. Indeed, both were abrogated in peritoneal macrophages from YTHDF3$^{-/-}$ *Ifnar1*$^{-/-}$ double knockout mice (Fig. 2*D* and *SI Appendix*, Fig. S3*L*). YTHDF3 knockdown in *Ifnar1*$^{-/-}$peritoneal macrophages had no effect on ISG expression and VSV replication (*SI Appendix*, Fig. S3 *J* and *K*), which further suggested that the activation of ISGs in the absence of YTHDF3 was dependent on IFNAR1 signaling. Altogether, our data demonstrate activation of ISGs via the IFNAR1 pathway in YTHDF3-deficient cells is responsible for the cell resistance to viral infection.

YTHDF3 Deficiency Protects Mice Against VSV Infection. To investigate the antiviral function of YTHDF3 in vivo, we challenged YTHDF3$^{-/-}$ mice with VSV via tail i.v. injection. We found that VSV replication and VSV titers in liver, spleen, and lung from YTHDF3$^{-/-}$ mice were significantly lower than the corresponding levels in WT mice (Fig. 3 *A* and *B*). As a result, YTHDF3$^{-/-}$ mice exhibited longer survival times (Fig. 3*D*) and showed reduced infiltration of inflammatory cells in the lung (Fig. 3*C*) after lethal VSV infection compared with the control groups. Thus, the loss of YTHDF3 protects mice against VSV infection.

YTHDF3 Promotes Translation of FOXO3 Through Binding to FOXO3 mRNA Independent of METTL3-Mediated m^{6}A. We next investigated the mechanism of antiviral resistance upon YTHDF3 loss. As previous studies have confirmed that the YTHDF3 binds to RNAs in vitro (16, 17, 27), we hypothesized that YTHDF3 might regulate ISG expression by directly binding to target RNAs. We first performed enhanced crosslinking and immunoprecipitation sequencing (eCLIP-seq) to identify transcriptome-wide YTHDF3-bound RNAs (28). Immunoblot analysis of protein-RNA complexes and YTHDF3 protein IP efficiency revealed extensive signals after IP in YTHDF3$^{+/+}$ RAW264.7 cells but not in YTHDF3$^{-/-}$ RAW264.7 cells (*SI Appendix*, Fig. S6 *A* and *B*). YTHDF3 preferentially bound the coding sequence and 3′ untranslated regions (UTRs) as previously reported (*SI Appendix*, Fig. S6*C*). The gene ontology (GO) analysis of YTHDF3-bound RNAs indicates that YTHDF3 might be involved in a variety of biological functions including transcription, RNA processing, translation initiation, and the immune system process (*SI Appendix*, Fig. S6*D*).

To further elucidate the mechanisms underlying YTHDF3-mediated inhibition of basal ISG expression, we focused on the regulators of IFN responses that showed considerable enrichment among YTHDF3-bound RNAs. However, we found that YTHDF3 did not directly bind to ISGs or to signaling factors of the JAK-STAT pathway and YTHDF3 did not affect the stability of ISG mRNAs (*SI Appendix*, Fig. S6*G*). Among the eCLIP-seq data, a transcription repressor FOXO3 was identified as a YTHDF3-bound RNA (over 16-fold enriched relative to size-matched input) (*SI Appendix*, Fig. S6*E*), which is known to negatively regulate ISG expression (29). The selective eCLIP interactions of YTHDF3 were found primarily to be with the translation initiation region of FOXO3 mRNA. The interaction was further analyzed by RNA IP and qPCR and confirmed that YTHDF3 binds to the FOXO3 transcript (Fig. 4*A*). We found that the lack of YTHDF3 specifically reduced FOXO3 protein expression without affecting the level of FOXO3 mRNA (Fig. 4*B*). Consistently, the low FOXO3 protein levels in YTHDF3$^{-/-}$ RAW264.7 cells were increased upon stable expression of FLAG-YTHDF3 (*SI Appendix*, Fig. S6*F*). However, we found that METTL3 did not have any effect on FOXO3 expression and YTHDF3 binding to FOXO3 mRNA (Fig. 4 *C* and *D*). These results indicated that YTHDF3 binds mRNA of the

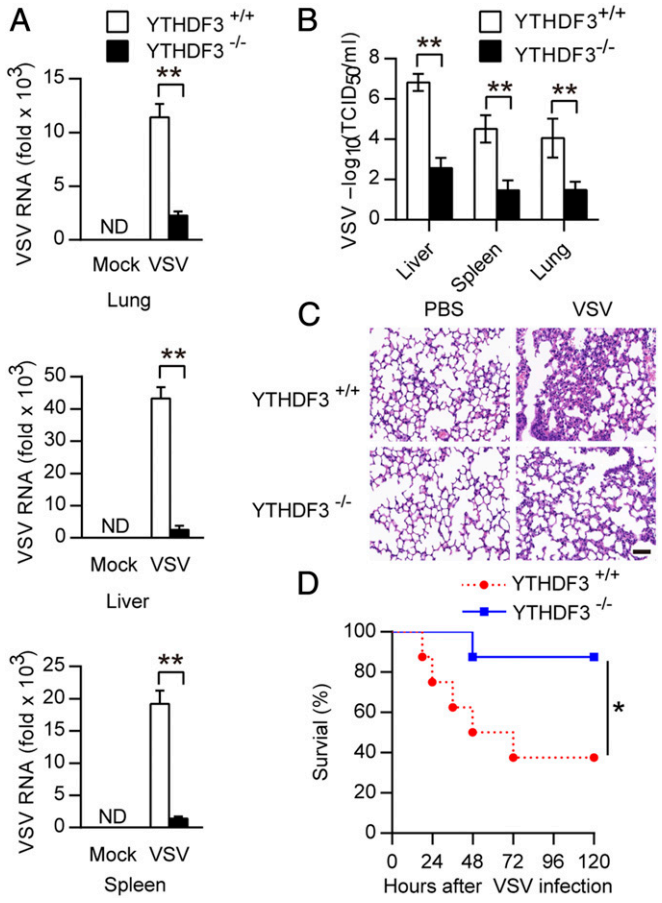

Fig. 3. YTHDF3$^{-/-}$ mice are more resistant to VSV infection. (*A*) YTHDF3$^{+/+}$ and YTHDF3$^{-/-}$ mice were i.v. injected with VSV for 24 h through the tail vein, then the levels of VSV RNA in the lung, liver, and spleen were analyzed by qPCR. (*B*) TCID50 assay was used to analyze VSV loads in the liver, spleen, and lung of the mice infected as in *A* ($n = 3$ per group). (*C*) YTHDF3$^{+/+}$ and YTHDF3$^{-/-}$ mice were i.v. injected with VSV for 24 h as in *A*, followed by hematoxylin-eosin staining of lung sections. (Scale bar, 50 μm.) (*D*) Survival of YTHDF3$^{+/+}$ and YTHDF3$^{-/-}$ mice ($n = 10$ per group) i.v. injected with VSV (5×10^8 pfu per mouse). Data are representative of three independent experiments [error bars (*A* and *B*), SD]. $^*P < 0.05$, $^{**}P < 0.01$ [two-tailed Student's *t* test (*A* and *B*) or Gehan-Breslow-Wilcoxon test (*D*)]. ND, not detectable.

repressive transcription factor FOXO3 and promotes the translation of FOXO3 independently of METTL3-mediated m^{6}A modification.

Both YTH and P/Q/*N*-Rich Domains of YTHDF3 Are Indispensable for Its RNA-Binding Capacity. To identify the FOXO3 RNA-binding domain of YTHDF3, we stably expressed YTHDF3 deletion mutants in RAW264.7 cells (*SI Appendix*, Fig. S7 *A* and *B*). We found that only full-length YTHDF3 could bind to FOXO3 mRNA. Deletion of either the YTH domain (△YTH) or the Pro/Gln/Asn-rich domain (△P/Q/*N*) of YTHDF3 abrogated binding to FOXO3 and other targets including LARP1 mRNA and SON mRNA (Fig. 4*E*). FOXO3 mRNA was enriched by the YTH domain by about 10-fold more than the △YTH mutant, but YTH alone did not regain the full ability of binding target RNAs (Fig. 4*E*).

As the YTH domain employs a conserved mechanism for recognizing RNA and crystal structures of YTHDF2 and YTHDC1 characterized several residues that are potentially important for m^{6}A-RNA recognition (30, 31), we generated four specific YTHDF3 mutants. The mutants were generated by the introduction of alanine at residues K422 and R533, which were found on the surface of YTH and were involved in binding to the RNA backbone, and at W438 and W492, which reside within the hydrophobic pocket for specific recognition of m^{6}A-modified RNA (*SI Appendix*, Fig. S7*C*). We found that all of these mutants abrogated YTHDF3 binding to FOXO3 mRNA (*SI Appendix*, Fig. S7*D*). These results indicate that the YTH domain and P/Q/*N*-rich domain of YTHDF3 are indispensable for effective YTHDF3-RNA interaction.

YTHDF3 Promotes Translation of FOXO3 to Inhibit ISG Expression by Synergistically Interacting with PABP1 and eIF4G2. To gain further insight into its mechanism of action, we analyzed YTHDF3 interacting partners by coimmunoprecipitation combined with protein mass spectrometry. A total of 141 proteins were found to interact with YTHDF3. We performed GO analysis and found that YTHDF3-interacting proteins are enriched in functional pathways related to translation, RNA processing, and RNA metabolism (*SI Appendix*, Fig. S8*A* and Table S2), supporting its known role as a regulator of translation, consistent with previous studies (16, 17). To study this further, we first confirmed the cytoplasmic location of YTHDF3 by immunofluorescence (*SI Appendix*, Fig. S8*B*). Next, we used polysome profiling and RT-PCR to examine the distribution of the endogenous YTHDF3 target FOXO3 mRNA in the ribosome fractions to quantify the proportion

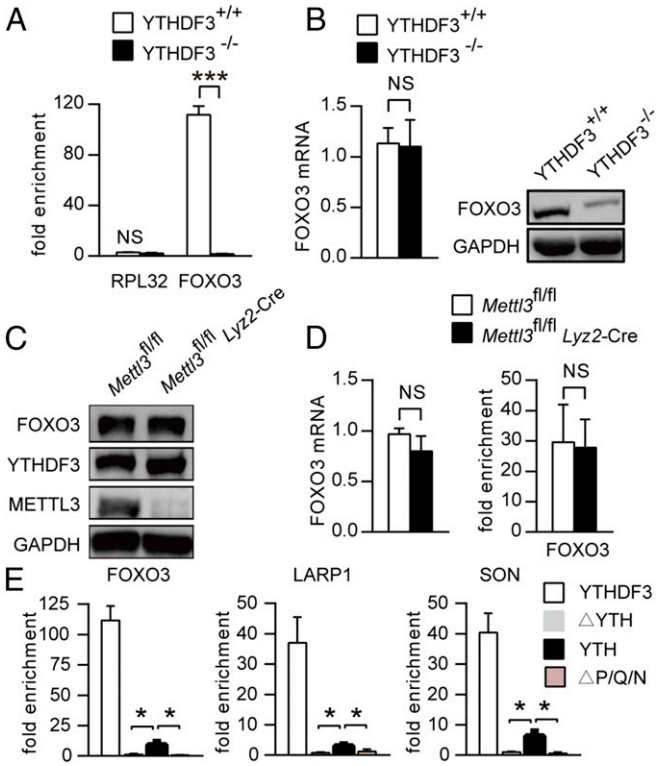

Fig. 4. YTHDF3 promotes translation of FOXO3 through binding to the translation initiation region of FOXO3 mRNA independently of METTL3-mediated m^{6}A. (*A*) Fold enrichment of RPL32 and FOXO3 by co-IP of YTHDF3 [RNA-binding protein IP (RIP)] with qPCR from YTHDF3$^{+/+}$ and YTHDF3$^{-/-}$ RAW264.7 cells. (*B*) qPCR and immunoblot analysis of FOXO3 mRNA and protein expression in YTHDF3$^{+/+}$ and YTHDF3$^{-/-}$ BMDMs. (*C*) Immunoblot analysis of FOXO3 expression in *Mettl3*$^{fl/fl}$ and *Mettl3*$^{fl/fl}$ *Lyz2*-Cre BMDMs. (*D*) qPCR analysis of FOXO3 mRNA in BMDMs as in *C*, and fold enrichment of FOXO3 by co-IP of YTHDF3 RIP with qPCR from *Mettl3*$^{fl/fl}$ and *Mettl3*$^{fl/fl}$ *Lyz2*-Cre BMDMs. (*E*) Fold enrichment of FOXO3, LARP1, and SON by RIP qPCR, from YTHDF3$^{-/-}$ RAW264.7 cells with stable expression of YTHDF3, △YTH, YTH, and △P/Q/*N*. $^*P < 0.05$, $^{***}P < 0.001$. NS, not significant.

that is translated. We found that the relative distribution of FOXO3 mRNA shifted from the polysome to the subpolysome fraction in YTHDF3$^{-/-}$ BMDMs (Fig. 5*A*). These results indicate that YTHDF3 promotes the translation of FOXO3 mRNA.

We next analyzed whether any partners of YTHDF3 cooperatively promoted the translation of FOXO3. We found that YTHDF3 directly interacted with PABP1 and eIF4G2 by IP using an anti-YTHDF3 antibody in RAW264.7 cells (Fig. 5*B*) and only full-length YTHDF3 could interact with PABP1 in HEK293T (*SI Appendix*, Fig. S8*C*). In addition, PABP1 could bind to FOXO3 mRNA (*SI Appendix*, Fig. S8*D*). Knockdown of either PABP1- or eIF4G2-inhibited FOXO3 protein levels (Fig. 5*C*) and consistent with these results, ISG expression was upregulated (*SI Appendix*, Fig. S8 *F* and *G*), and VSV infection was inhibited (*SI Appendix*, Fig. S8*E*). Together, these results indicate that YTHDF3 promotes the translation of FOXO3 to inhibit ISG expression by cooperating with PABP1 and eIF4G2.

FOXO3 Is Pivotal in YTHDF3-Mediated Negative Regulation of Antiviral Innate Immunity. To determine whether YTHDF3 negatively regulates innate antiviral immunity through promoting translation of FOXO3, we performed siRNA knockdown of FOXO3 and a rescue assay in YTHDF3$^{-/-}$ mouse embryonic fibroblasts (MEFs). We found that siFOXO3 enhanced IFIT1 and IRF7 mRNA expression (Fig. 6*A* and *SI Appendix*, Fig. S8*H*) as described previously (32). Fluorescence microscopy showed that the replication of VSV GFP was inhibited by siFOXO3 in peritoneal macrophages from *Ifnar1*$^{+/+}$ mice but not in *Ifnar1*$^{-/-}$ peritoneal macrophages (Fig. 6*B*). This further suggests that FOXO3 inhibits antiviral innate immunity via suppression of IFNAR1 signaling. Finally, we transfected FOXO3 into YTHDF3$^{-/-}$ MEFs and found that it restored VSV-G protein expression (Fig. 6*C*). Taken together, our data demonstrate that FOXO3 is required for YTHDF3-mediated negative regulation of antiviral innate immunity via suppression of ISG expression.

Discussion

IFN-mediated innate immune responses are hardwired within genomes and constitute the primary line of defense against viruses. Upon viral infection, host signaling cascades are triggered to induce robust IFN production. Thousands of ISGs are induced by the JAK-STAT pathway. The host manipulates these ISGs to restrain different steps of the viral life cycle. Most host cell types can respond to low levels of endogenous IFN-I under homeostatic conditions, which maintain ISG expression. However, very little is known about whether IFN production- and signaling-dependent activations of ISGs occur in the absence of viral infection and how it is regulated. Here, we revealed a translation control model of YTHDF3-mediated suppression of ISG expression and demonstrated a previously unknown in vivo physiological function of YTHDF3 in regulating antiviral innate responses.

YTHDF3 regulated the translation and decay of mRNAs through cooperation with YTHDF1 and YTHDF2 (16, 17). In addition, YTHDF1 and YTHDF3 have been reported to negatively affect each other's RNA-binding affinity (16). Here, we found that only YTHDF3 deficiency promoted basal ISG expression through inhibiting the translation of FOXO3. Although YTHDF1 and YTHDF2 both bind to FOXO3 mRNA, according to published data (13, 14), neither affected host innate antiviral responses. Thus, RNA binding of YTHDF proteins is not sufficient for them to function in the regulation of antiviral immunity, which may need other factors to work together.

Selective translation is known to be important for antiviral innate immunity. Specifically, deficiency of the eukaryotic translation initiation factor 4E-binding proteins 4E-BP1 or 4E-BP2 in MEFs enhanced translation of the transcription factor IRF7 mRNA, which has a long and highly structured 5′ UTR and, consequently, increased the antiviral innate response (33). Accurate and efficient translation has also been shown to be regulated by m^{6}A-mRNA modifications. Specifically, YTHDF1, YTHDF3, and IGF2BP1 promote translation efficiency by binding to the 3′ UTR of m^{6}A-modified mRNA, whereas eIF3 enhanced translation activation by binding to 5′ UTR (34). In addition, eIF4G is a subunit of the eukaryotic translation initiation 4F (eIF4F) complex and a large scaffolding protein, which interacts with eIF4E, eIF4A, and PABP to assemble a mRNA "closed loop." The circularization of 5′ UTR and poly(A) tail can promote mRNA stability and translation (35). Here, we propose a translation control mode whereby YTHDF3 promotes translation through binding to the translation initiation region of

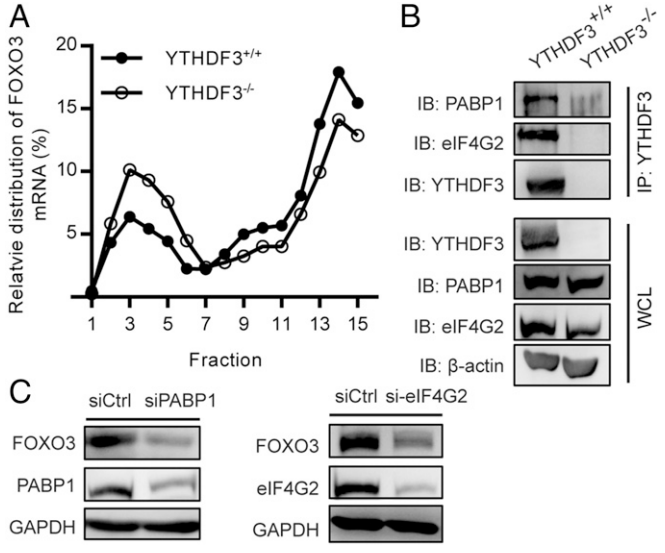

Fig. 5. YTHDF3 promotes the translation of FOXO3 by cooperating with PABP1 and eIF4G2. (*A*) qPCR analysis of FOXO3 in YTHDF3$^{+/+}$ and YTHDF3$^{-/-}$ BMDMs, fractioned into polysomes. (*B*) Cell lysates were IP using an anti-YTHDF3 antibody, followed by immunoblot analysis using the indicated antibodies. (*C*) Immunoblot analysis of indicated proteins in lysates of primary peritoneal macrophages transfected with siCtrl, siPABP1, or si-eIF4G2.

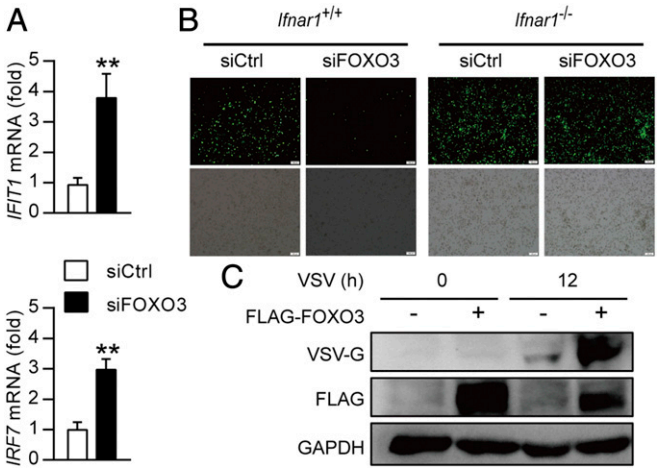

Fig. 6. YTHDF3 suppresses IFN-I-mediated antiviral innate immunity via upregulation of FOXO3 protein expression. (*A*) qPCR analysis of IFIT1 and IRF7 mRNAs under siFOXO3 versus siCtrl. (*B*) Fluorescence (*Top*) and bright field (*Bottom*) microscopy of mouse peritoneal macrophages from *ifnar1*$^{+/+}$ and *ifnar1*$^{-/-}$ mice transfected with siCtrl and siFOXO3, infected for 12 h with VSV GFP (green fluorescence) (MOI, 1). (*C*) Immunoblot analysis of VSV-G protein in YTHDF3$^{-/-}$ MEFs transfected with FOXO3. $^{**}P < 0.01$.

FOXO3 mRNA, in cooperation with PABP1 and eIF4G2, possibly by RNA looping.

Crystal studies revealed that the YTH domain recognizes m^6A by an aromatic cage (30). We found that YTHDF3 mutants, △YTH, △P/Q/*N*, K422A, R533A, W438A, and W492A abrogated its RNA-binding capacity, indicating that the intact YTHDF3 protein was required for binding. The current results suggest that YTHDF3 can regulate the translation of FOXO3 in the absence of m^6A introduced by METTL3. However, the other m^6A methyltransferases may influence the function of YTHDF3. An alternative mechanism was suggested by a recent report showing that YTHDF1-3 and YTHDC1 could bind directly also to N^1-methyladenosine- (m^1A-) modified RNAs (32). W432 in YTHDF2, which is a conserved residue similar to W438 in YTHDF3, was also required for its recognition of m^1A. Previous studies have shown that m^1A, around the start codon, is also involved in mRNA translation (36). Nevertheless, it remains possible that YTHDF3 affects translation via binding to different mRNA modifications on the transcripts. Therefore, single-nucleotide-resolution mappings of YTHDF3-bound RNA modifications are required in future experiments to provide more insight into selective translation regulation by YTHDF3. Altogether, YTHDF3 appears to be multifunctional with its function determined by different partners and/or in different cell types.

There have been numerous studies demonstrating the importance of the virus epitranscriptome for infection. For example, modified viral RNAs, such as m^6A, 5-methylcytidine, pseudouridine (Ψ), 2-thiouridine, and 5-methyluridine, inhibit antiviral immunity (25, 26), and RNA and DNA viruses undergo epitranscriptome reprogramming upon infection. Indeed, viral infection also resulted in a dynamic change in host RNA modifications, particularly of transcripts related to viral replication and immune responses. Here, we found up-regulated ISG expression in YTHDF3-deficient immune cells in the absence of infection. Therefore, we focused on the role of YTHDF3 in host gene expression under homeostatic conditions.

Our paper also could raise the possibility for disease relevance, such as autoimmune disorders and tumors with aberrant IFN signatures, which could be the result of dysregulation of YTHDF3 expression or function. In conclusion, we have identified YTHDF3 as a negative regulator of ISG expression, through promoting the translation of FOXO3 under homeostatic conditions. These results confirm that YTHDF3 plays vital roles in the translation control of antiviral innate responses. The roles of YTHDF3 in the pathogenesis of IFN-dysregulated inflammatory autoimmune diseases needs further investigation.

Materials and Methods

Mice. All animal experiments were performed in accordance with the National Institutes of Health *Guide for the Care and Use of Laboratory Animals* (37), with the approval of the Scientific Investigation Board of Chinese Academy of Medical Sciences (ACUC-A02-2016-015). $YTHDF3^{-/-}$ mice were generated using the CRISPR-Cas9 system. All mice information is described in *SI Appendix, Materials and Methods*.

RIP-qPCR. This procedure was adapted from a published report (4). For comparison of the RNA-binding protein ability, relative enrichment was first normalized to input and then analyzed by comparison with the data from the sample IPed with the indicated antibody.

Statistical Analysis. Statistical significance between two-group comparisons was analyzed by a two-tailed Student *t* test. The statistical significance of survival curves was compared with the generalized Wilcoxon test. The value of $P < 0.05$ was considered statistically significant.

ACKNOWLEDGMENTS. This work was supported by grants from the National Natural Science Foundation of China (81788101, 31390431), the National Key Research & Development Program of China (2018YFA0507403), and the Chinese Academy of Medical Sciences Innovation Fund for Medical Sciences (2016-12M-1-003).

1. Zhao BS, Roundtree IA, He C (2017) Post-transcriptional gene regulation by mRNA modifications. *Nat Rev Mol Cell Biol* 18:31–42.
2. Hsu PJ, Shi H, He C (2017) Epitranscriptomic influences on development and disease. *Genome Biol* 18:197.
3. Li HB, et al. (2017) m^6A mRNA methylation controls T cell homeostasis by targeting the IL-7/STAT5/SOCS pathways. *Nature* 548:338–342.
4. Zheng Q, Hou J, Zhou Y, Li Z, Cao X (2017) The RNA helicase DDX46 inhibits innate immunity by entrapping m^6A-demethylated antiviral transcripts in the nucleus. *Nat Immunol* 18:1094–1103.
5. Kennedy EM, Courtney DG, Tsai K, Cullen BR (2017) Viral epitranscriptomics. *J Virol* 91: e02263-16.
6. Schneider WM, Chevillotte MD, Rice CM (2014) Interferon-stimulated genes: A complex web of host defenses. *Annu Rev Immunol* 32:513–545.
7. Ivashkiv LB, Donlin LT (2014) Regulation of type I interferon responses. *Nat Rev Immunol* 14:36–49.
8. Crow YJ (2015) Type I interferonopathies: Mendelian type I interferon up-regulation. *Curr Opin Immunol* 32:7–12.
9. Iwata S, et al. (2017) The transcription factor T-bet limits amplification of type I IFN transcriptome and circuitry in T helper 1 cells. *Immunity* 46:983–991.e4.
10. Chen K, et al. (2017) Methyltransferase SETD2-mediated methylation of STAT1 is critical for interferon antiviral activity. *Cell* 170:492–506.e14.
11. Piccirillo CA, Bjur E, Topisirovic I, Sonenberg N, Larsson O (2014) Translational control of immune responses: From transcripts to translatomes. *Nat Immunol* 15:503–511.
12. Patil DP, Pickering BF, Jaffrey SR (2018) Reading m^6A in the transcriptome: m6A-binding proteins. *Trends Cell Biol* 28:113–127.
13. Wang X, et al. (2015) N^6-methyladenosine modulates messenger RNA translation efficiency. *Cell* 161:1388–1399.
14. Wang X, et al. (2014) N6-methyladenosine-dependent regulation of messenger RNA stability. *Nature* 505:117–120.
15. Du H, et al. (2016) YTHDF2 destabilizes m(6)A-containing RNA through direct recruitment of the CCR4-NOT deadenylase complex. *Nat Commun* 7:12626.
16. Li A, et al. (2017) Cytoplasmic m^6A reader YTHDF3 promotes mRNA translation. *Cell Res* 27:444–447.
17. Shi H, et al. (2017) YTHDF3 facilitates translation and decay of N^6-methyladenosine-modified RNA. *Cell Res* 27:315–328.
18. Gokhale NS, et al. (2016) N6-methyladenosine in Flaviviridae viral RNA genomes regulates infection. *Cell Host Microbe* 20:654–665.
19. Lichinchi G, et al. (2016) Dynamics of human and viral RNA methylation during Zika virus infection. *Cell Host Microbe* 20:666–673.
20. Courtney DG, et al. (2017) Epitranscriptomic enhancement of influenza A virus gene expression and replication. *Cell Host Microbe* 22:377–386.e5.
21. Tan B, et al. (2018) Viral and cellular N^6-methyladenosine and N^6,2′-O-dimethyladenosine epitranscriptomes in the KSHV life cycle. *Nat Microbiol* 3:108–120.
22. Kennedy EM, et al. (2016) Posttranscriptional m^6A editing of HIV-1 mRNAs enhances viral gene expression. *Cell Host Microbe* 19:675–685.
23. Lichinchi G, et al. (2016) Dynamics of the human and viral m(6)A RNA methylomes during HIV-1 infection of T cells. *Nat Microbiol* 1:16011.
24. Tirumuru N, et al. (2016) N(6)-methyladenosine of HIV-1 RNA regulates viral infection and HIV-1 Gag protein expression. *eLife* 5:e15528.
25. Karikó K, Buckstein M, Ni H, Weissman D (2005) Suppression of RNA recognition by Toll-like receptors: The impact of nucleoside modification and the evolutionary origin of RNA. *Immunity* 23:165–175.
26. Durbin AF, Wang C, Marcotrigiano J, Gehrke L (2016) RNAs containing modified nucleotides fail to trigger RIG-I conformational changes for innate immune signaling. *MBio* 7:e00833-16.
27. Zhang Z, et al. (2010) The YTH domain is a novel RNA binding domain. *J Biol Chem* 285:14701–14710.
28. Van Nostrand EL, et al. (2016) Robust transcriptome-wide discovery of RNA-binding protein binding sites with enhanced CLIP (eCLIP). *Nat Methods* 13:508–514.
29. Litvak V, et al. (2012) A FOXO3-IRF7 gene regulatory circuit limits inflammatory sequelae of antiviral responses. *Nature* 490:421–425.
30. Xu C, et al. (2014) Structural basis for selective binding of m6A RNA by the YTHDC1 YTH domain. *Nat Chem Biol* 10:927–929.
31. Zhu T, et al. (2014) Crystal structure of the YTH domain of YTHDF2 reveals mechanism for recognition of N6-methyladenosine. *Cell Res* 24:1493–1496.
32. Dai X, Wang T, Gonzalez G, Wang Y (2018) Identification of YTH domain-containing proteins as the readers for N1-methyladenosine in RNA. *Anal Chem* 90:6380–6384.
33. Colina R, et al. (2008) Translational control of the innate immune response through IRF-7. *Nature* 452:323–328.
34. Meyer KD, et al. (2015) 5′ UTR m^6A promotes cap-independent translation. *Cell* 163: 999–1010.
35. Chu J, Cargnello M, Topisirovic I, Pelletier J (2016) Translation initiation factors: Reprogramming protein synthesis in cancer. *Trends Cell Biol* 26:918–933.
36. Dominissini D, et al. (2016) The dynamic N(1)-methyladenosine methylome in eukaryotic messenger RNA. *Nature* 530:441–446.
37. National Research Council (2011) *Guide for the Care and Use of Laboratory Animals* (National Academies Press, Washington, DC), 8th Ed.